Power Management System with Load Power Regulation for Zonal Secondary DC-Grids Survivability: A Load Priority-Based Approach

B Wingelaar[1] MSc

J J Deroualle[2] MSc IEEE Member

[1] *Royal IHC, Research & Development Dept., NL*
[1] *Corresponding Author. Email: b.wingelaar@royalihc.com*

[2] *Royal IHC, FD Engineering Dept., NL*
[2] *Corresponding Author. Email: jj.deroualle@royalihc.com, jacques.deroualle@ieee.org*

Synopsis

This article proposes an algorithm based on load priorities to ensure survivability in shipboard zonal secondary DC-grids. The transition to alternative fuels introduces new opportunities and new challenges. Using inherent DC power electronics for integrating energy storage systems (ESSs) and renewable energy sources (RESs) demands novel control mechanisms for dealing with power converter overload conditions. In that sense, the power management system (PMS) has to incorporate active load management systems to ensure the continuous operation of essential loads when the ship is operating in critical missions or during abnormal power situations. This work employs the concept of a zonal DC secondary distribution network, which is based on the insertion of supercapacitors for voltage time constant enhancement. This grid concept is used to formulate the survivability objective as a DC-link voltage recovery function, with a minimum operation voltage that must not be exceeded whilst sustaining continuous operation whenever feasible. That is relevant for short-circuit currents and underestimated and unforeseen high peak loads. In these cases, the load demand may exceed the nominal ratings of the DC/DC converter that feeds the secondary zone load. Moreover, the power converter may suddenly become unavailable. Then, supercapacitors can provide the additional power, enabling the momentary survivability of the zonal secondary grid. However, in this process, the DC-link voltage value decreases while the ESS is discharged. The power imbalance can only be sustained for a limited period, determined by the supercapacitor's initial operation conditions. If the DC voltage limit is exceeded, load reduction is required to counterbalance the load mismatch and ensure voltage recoverability. A load priority approach is applied in this article to meet the load reduction objective, with essential and emergency loads having the highest priority. A study case is proposed using time-domain simulations in a Matlab-Simulink environment to demonstrate the load management functionality. The results show that supercapacitors and load management substantially increase the survivability of the zonal secondary load centre whenever one of the DC/DC converters fails during operation.

Keywords: Load management system; Zonal electrical distribution system; DC secondary distribution system; Supercapacitor network; Survivability; Multi-agent system

1. Introduction

One of the benefits of a power converter's integration into DC-grids is to optimise the power equipment space and weight constraints onboard. In that sense, it might get impractical to oversize power converters for obtaining high survivability rates under critical missions – it becomes evident that inverter-based resources (IBRs) may easily be overloaded when supplying impulsive loads for navy purposes, for example. ESS implementation is imperative for DC-grid's high performance; however, their size, weight and potential hazards limit their extensive use on ships (Du et al., 2019). To keep the system stable for a wide range of power demands (and de-rated events), it is advisable to incorporate load management to deal with the load balance in real-time and complicated fluctuating power requirements (Du et al., 2019). The present paper will discuss the implementation of such power regulation for a zonal secondary grid design based on supercapacitor's application.

This article is organised as follows. In Section 2, the supercapacitor zonal secondary DC distribution is introduced as the basis of our study. There are also some insights about the chopper controlling when energy storage devices are directly connected to the DC-link. Section 3 depicts the multi-agent system and its group objective to mind the self-restoration functionality in a secondary distribution grid. Section 4 proposes a study case for assessing the suggested power regulation – the component modelling and logic control algorithm are

Author's Biography
Bart Wingelaar is a R&D engineer at Royal IHC. He studied at the Eindhoven University of Technology, The Netherlands, and has a background in control engineering, dynamical systems, optimization, and optimal control strategies.
Jacques Julien Deroualle is current a Project Engineer at Royal IHC in Kinderdijk, NL. He obtained his Master Degree of Science at Politecnico di Milano in 2018. His main working interests include HV/MV power systems, propulsion electric drives, DC-grids, shore connection, zero-emission vessels, and energy storage systems. He is a member of the Working Group of IEEE Standard P45.1 'Recommended Practice for Electrical Installations on Shipboard Design'.

 https://doi.org/10.24868/11136

given. Then, a brief discussion about the improvement in survivability is presented. Finally, conclusions and future research topics are stated in Section 5.

2. Supercapacitor zonal secondary DC distribution

This paper focuses on a secondary DC-Grid design part of a Zonal Electrical Distribution System (ZEDS). This grid type applies not only to all-electric ships but also to hospitals, airports, data centres, etc. This network concept permits the enhancement of the ship's survivability to adverse events (Bosich et al., 2023) that might be external to the electrical system itself but with direct consequences on the electrical operation (Deroualle & Vinks, 2024). A representative single-line diagram (SLD) of this network can be seen in Figure 1.

A shipboard ZEDS consists of different load zones supplied by two different connections into the primary distribution system and managed independently (Xu et al., 2022). The ring structure – from which the power generation and load subsystems are operated – is formed by port and starboard DC buses that run longitudinally along the ship and are connected by bow and stern cross-hull links (IEEE Std. 1709-2018). When a short circuit occurs in one of the main buses, the secondary loads within the zones will shift their power source of supply – automatically or manually – to the section unaffected by the electrical event (Xu et al., 2022). In that way, a ring communication network is expected to allow protection coordination and selectivity along the structure areas (Xu et al., 2022).

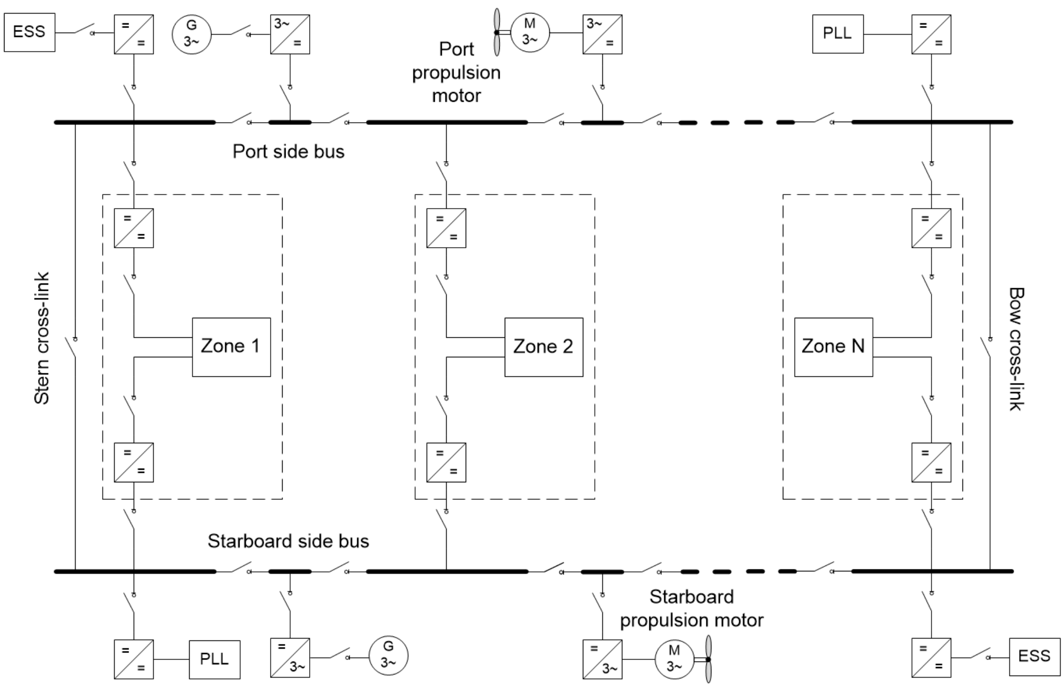

Figure 1: SLD representation of a shipboard power system based on ZEDS (Deroualle & Vinks, 2024)

In navy vessels, the emerging pulsed-power loads (PLLs) can be directly placed in the main distribution ring (Xu et al., 2022) or as part of the *N* load zones indicated in Figure 1. The last, at some extent of power, is achievable with DC/DC converters that would step down the voltage from 1 kV to 700 V, for example – this allows the use of ESSs to directly power the vital loads under the zones (Qazi et al., 2023).

Supercapacitors applied directly in the zonal low-voltage (LV) DC-links could provide more voltage inertia and increase the performance and stability of such PLLs. Moreover, it would unlock the possibility of implementing mechanical circuit breakers (MCBs) due to reducing the rate of change of the voltage (RoCoV) – in case of fault or transient events – and the voltage auto-recovery process once the electrical event is over (Deroualle & Vinks, 2024). This statement is valid as long as the short circuit levels are inside the withstand limits of the breaker technology, and the supercapacitor aftermath state of charge (SoC) is higher than 40% (or a pre-settled limit that enables the system to continue operation).

The zonal secondary DC distribution based on DC-link supercapacitors and MCB protection will imply some properties to the LV feeder circuits:

- The fault current will last for several seconds, making possible the time-current curve (TCC) selectivity approach between the protection apparatus;

- Once the faulty section is isolated from the rest of the grid, the voltage is automatically raised to the level in accordance with the supercapacitor SoC final condition;
- The supercapacitor's non-linearity will influence the network short-circuit currents to behave in an overdamped mode (smoothing the current waveform over time).

If a zonal DC/DC converter fails, the supercapacitor modules will continue to power the remaining base loads for a limited period (tens of seconds). That interval should be sufficient for the PMS to acknowledge the de-rated situation and proceed with countermeasures to assure the shipboard power system survivability (or at least partially). The coming sections will discuss such actions based on a zonal distribution example for the Dutch 'Seagoing Auxiliary Vessel'.

2.1. Auxiliary vessel secondary grid design

Figure 2 proposes the concept of a zonal secondary DC grid for the 'Seagoing Auxiliary Vessel' – this example, in particular, will not accommodate low-power PLLs. Thus, it will supply normal auxiliary loads through two 700 V busbars (open bus-tie breaker) for the principal machinery equipment (e.g., fuel transfer pumps, cooling water pumps, supply fans, heat recovery systems, etc); two 350 V busbars for lighting and DC accommodation loads; and one 700 V battery system for emergency loads (e.g., lighting, bilge/ballast pumps, etc).

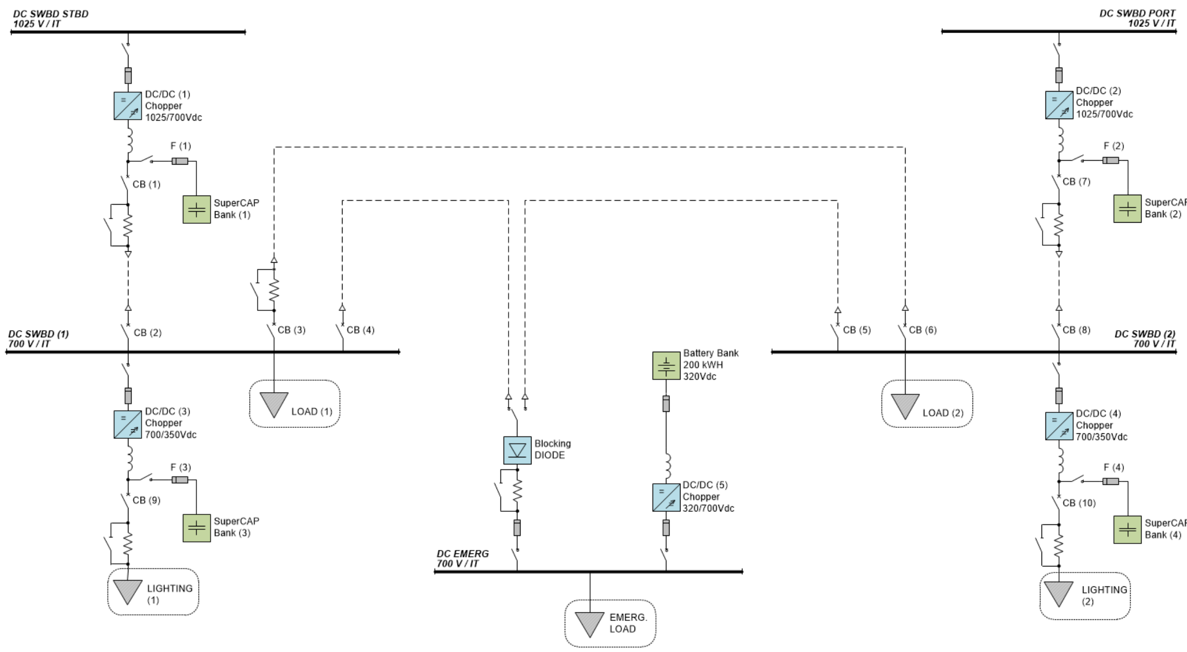

Figure 2: SLD representation for the 'Seagoing Auxiliary Vessel' secondary DC grid (Deroualle & Vinks, 2024)

The power system's data are displayed in Tables 1-3. The DC/DC choppers are expected to operate with a switching frequency of 5 kHz and an air-cooled method. The MCB feeders incorporate a switching by-pass resistance to limit the inrush currents when connecting two DC buses with different voltage levels. For example, in the 700 V bus-tie case, the power resistor has a nominal value of 0.05 Ω and a by-passing time of 3 seconds. The worst situation for closing the bus-tie 'CB (3)' would succeed when the converter 'DC/DC (1)' has failed – previously operating with full power – and when the busbar 'DC SWBD (1)' reaches the under-voltage limit of 620 V due to the 'SuperCAP Bank (1)' constant supply discharging for the local loads. The bus-tie transient current would peak at 886 A with a total energy dissipation of 65.6 kJ (Figure 3).

Table 1: Supercapacitor bank Power Ratings

Equipment	**Nominal Voltage (V)**	**Capacitance (F)**	**Nominal Current (A)**	**ESR @25°C (mΩ)**
SuperCAP (1) SuperCAP (2)	780	31.25	300	18-56
SuperCAP (3) SuperCAP (4)	390	20.83	100	27-84

Table 2: Chopper converter Power Ratings

Equipment	Input Nominal Voltage (V)	Output Voltage Range (V)	DC-link Power (kW)	Filter Inductance (μH)
DC/DC (1) DC/DC (2)	1025	640-760	149	(3x) 1640
DC/DC (3) DC/DC (4)	700	320-400	20	(3x) 3500
DC/DC (5)	320	640-760	124	(3x) 443

Table 3: Mechanical circuit breaker Power Ratings

Equipment	Number of Poles	Rated Current (A)	Operational Voltage (V)	Icu (kA) Ics (%Icu)
CB (1), CB (2) CB (7), CB (8)	4	400	750	36 (100%)
CB (3) CB (6)	4	320	750	36 (100%)
CB (4) CB (5)	4	100	750	36 (100%)
CB (9) CB (10)	2	175	500	36 (100%)

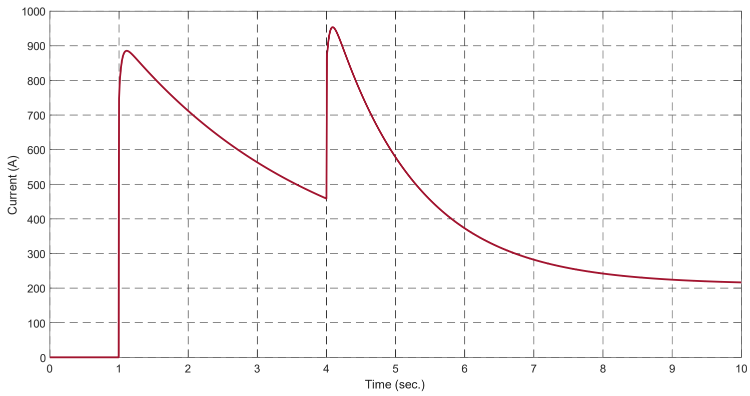

(a)

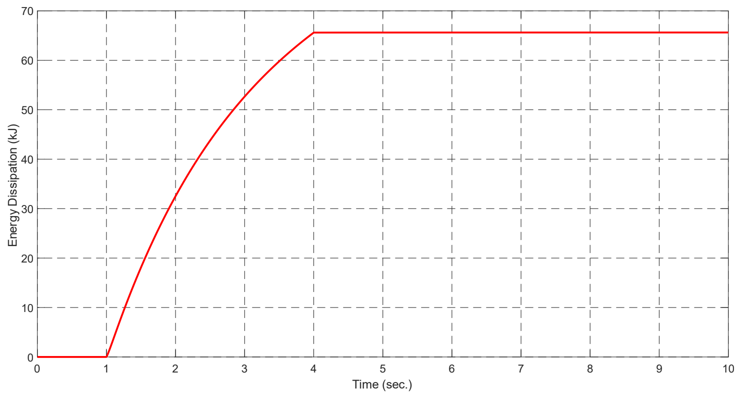

(b)

Figure 3: Bus-tie MCB by-pass closing operation
(a) DC feeder current (b) Resistor dissipated energy

 https://doi.org/10.24868/11136

Figure 4 (a) exbibits the total DC fault current at ‘DC SWBD (1)’ when the bus-tie breaker ‘CB (3)’ is closed (Deroualle & Vinks, 2024). In this example, it is considered that the fault contributions from main and lighting circuits to be zero – the converters ‘DC/DC (1)’ and ‘DC/DC (2)’ have the capability of interrupting the short-circuit current at the very initial stage; the upper high-speed fuses from ‘DC/DC (3)’ and ‘DC/DC (4)’ will limit to few milliseconds the downstream contribution current. The equivalent *L/R* circuit constant is lower than 5 ms with a peak current of 25.7 kA. The supercapacitors presence will increase the DC-link resultant fault to several seconds, which can create considerable arc-flash levels in the front of the power cabinets (Deroualle & Vinks, 2024). Thus, backup safeguarding fuses ‘F (1)’, ‘F (2)’, ‘F (3)’, and ‘F (4)’ are implemented for limiting the let-through energy. The correct fuse size has to consider the required time for making possible selectivity between the downstream network breakers (Deroualle & Vinks, 2024).

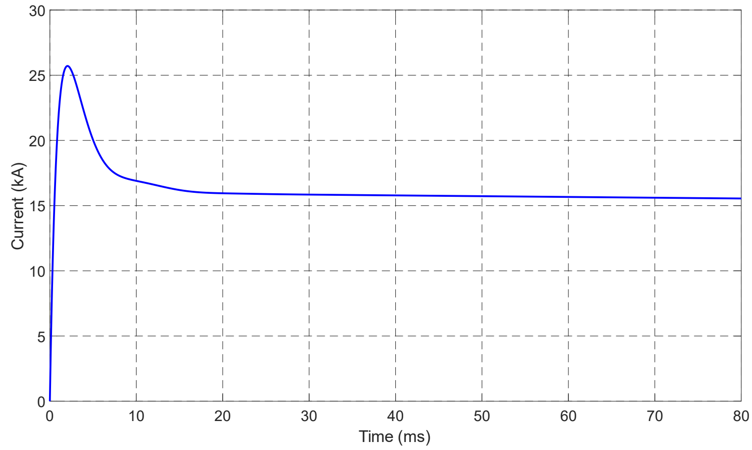

(a)

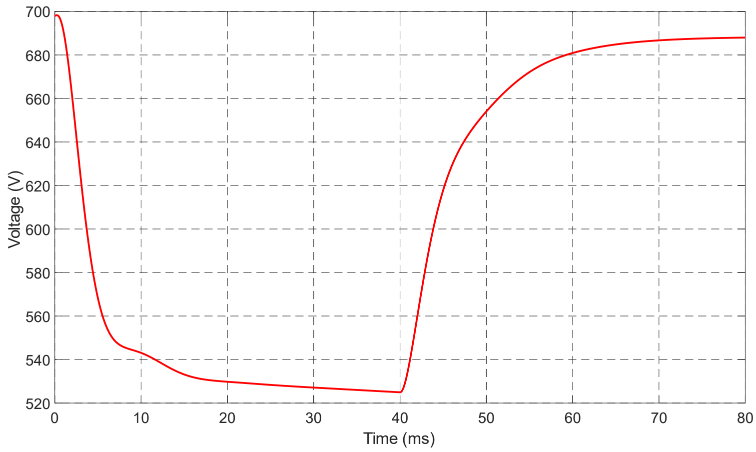

(b)

Figure 4: Fault level at DC-link ‘DC SWBD (1)’ (Deroualle & Vinks, 2024)
(a) Short-circuit current (b) Supercapacitor terminal voltage with 40 ms fault extinguish time

In the secondary circuit branch supplied by the bus ‘DC SWBD STBD’, the breaker ‘CB (1)’ – with a nominal current of 400 A (Table 3) – can be selected together with ‘F (1)’ gBat fuse-link of 500 A. The TCC chart of both protection apparatus is displayed in Figure 5. Considering the example of Figure 4, the ‘SuperCAP (1)’ current would merge the gBat fuse at instant ~80 ms, and instantaneously trip the ‘CB (1)’ – opening time estimated in the range of 20-40 ms according to common manufacturer values. The terminal voltage at the ‘SuperCAP (1)’ with fault extinction of 40 ms is shown in Figure 4 (b); the voltage auto-recovery property is the key feature that enables the survivability enhancement of the zonal secondary DC-grid with supercapacitors. Moreover, the chopper overload current curves – depending on the voltage trigger level – will be explained in the next sections; the breaker ‘CB (1)’ must be sized accordingly to allow the ‘SuperCAP (1)’ to supply overload conditions for a limited period of time.

 https://doi.org/10.24868/11136

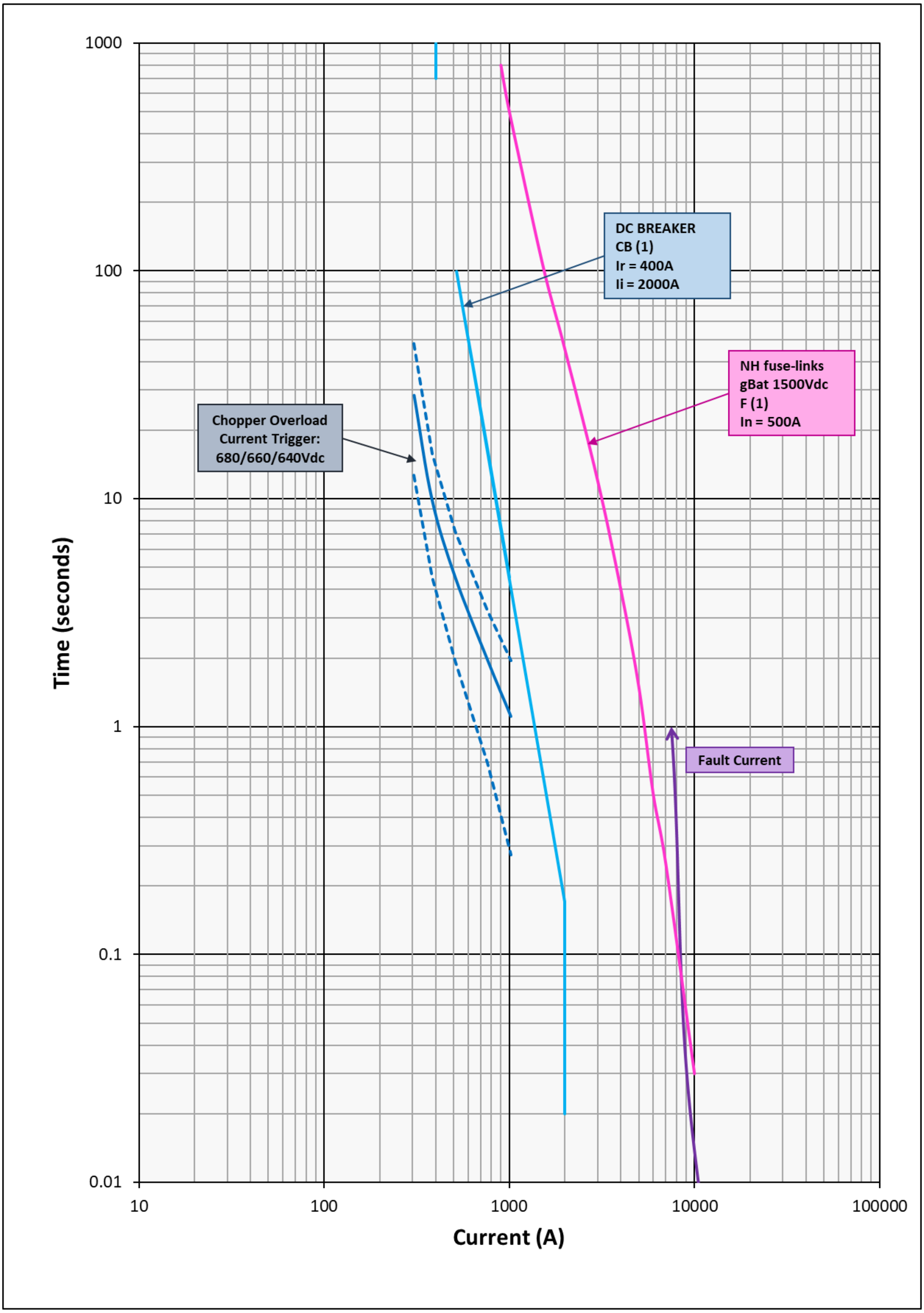

Figure 5: TCC chart for protection selectivity between 'CB (1)' and 'F (1)' protection devices.

https://doi.org/10.24868/11136

2.2. DC/DC chopper controlling

The zonal primary chopper converters (1025/700 V) are based on the ‘Average current-mode’ (ACM) control philosophy. Figure 6 presents a representation of the converter controlling scheme. This popular programming technique contains an average current loop compensator around a duty-cycle-controlled converter (Erickson & Maksimović, 2020). Furthermore, an outer voltage control loop is also closed around the ACM scheme. Figure 7 shows the block diagrams that model the ACM-controlled drive (Erickson & Maksimović, 2020).

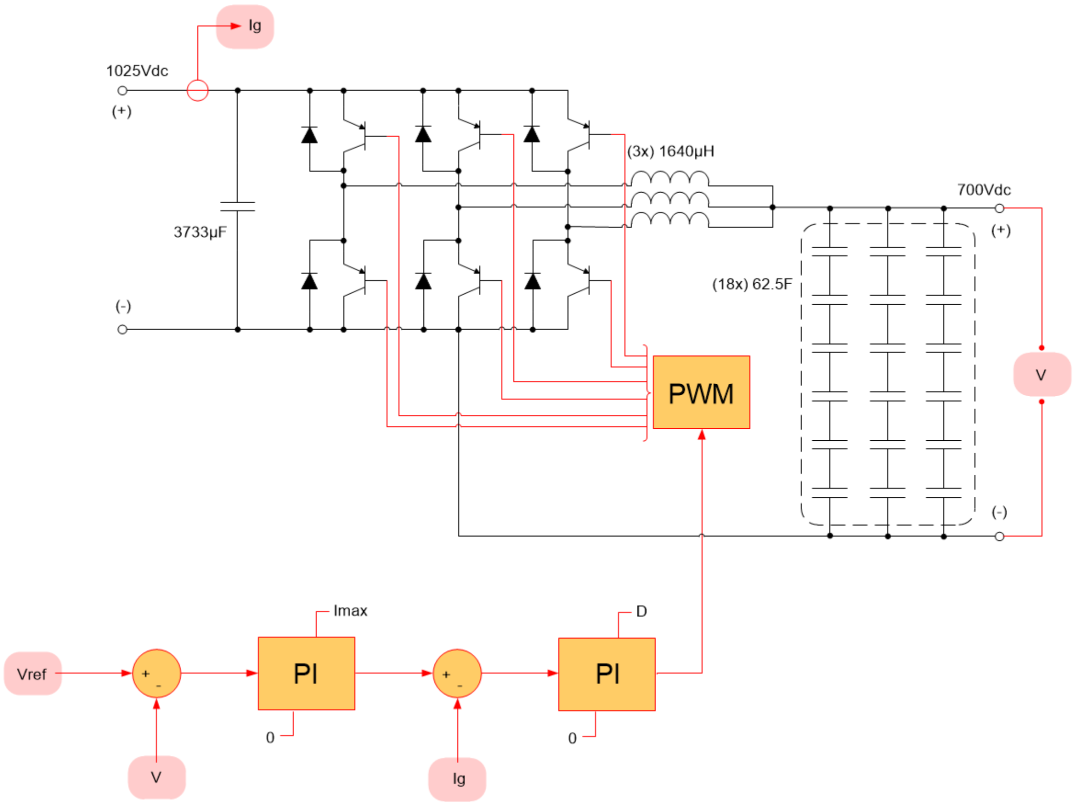

Figure 6: Zonal primary chopper converters (1025/700 V) controlling representation

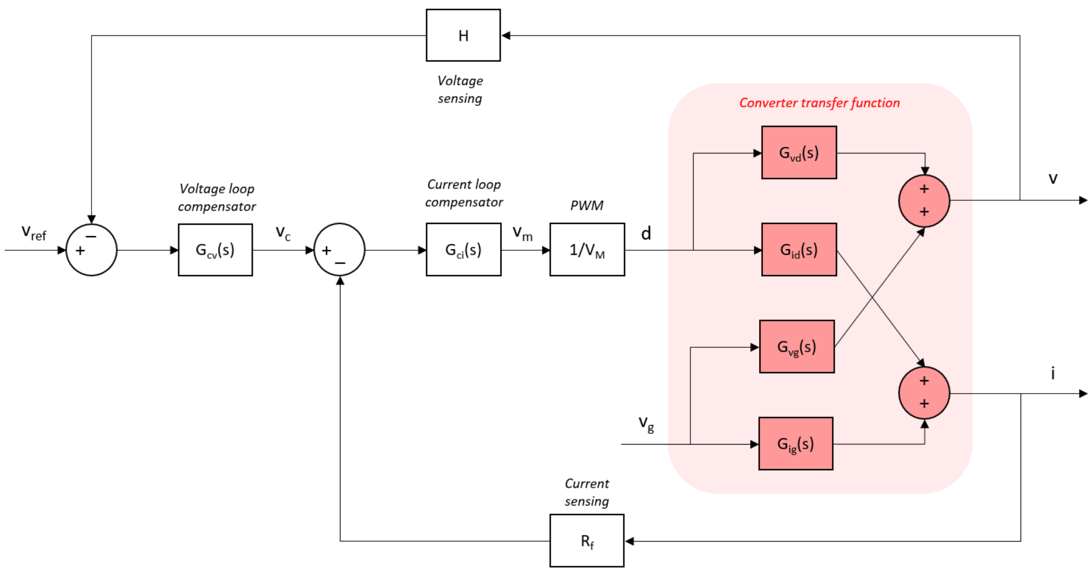

Figure 7: Block diagrams model of the ACM-controlled chopper (Erickson & Maksimović, 2020)

In Figure 7, a sensed output voltage *H* is compared to a reference signal V_{ref}, and the generated error signal is processed through a voltage loop compensator $G_{cv}(s)$, which will create a V_c current reference for the current control loop (Erickson & Maksimović, 2020). This reference point is compared to a sensed current signal R_f, and the outcome error is handled by a current loop compensator $G_{ci}(s)$ (Erickson & Maksimović, 2020). Finally, the Pulsed-Width Modulation (PWM) develops a switch control signal with duty cycle *d* to be applied to the chopper drive (Erickson & Maksimović, 2020).

The three inverter legs depicted in Figure 6 are separately controlled with a pulse-width modulation (PWM) signal that is 120° phase shifted, characterised by an 'Interleaved Current Control' mechanism. Therefore, a three-winding core choke is used to obtain a reduced ripple current at the output of the buck operating converter in the most efficient way.

The chopper is designed to have a crossover frequency of 500 Hz (one-tenth of the switching frequency) and a current loop phase margin equal to 73°. Following this reasoning, the voltage loop compensator is settled to have a crossover frequency of 50 Hz and a phase margin of 78° – the resulting voltage loop gain is shown in Figure 8.

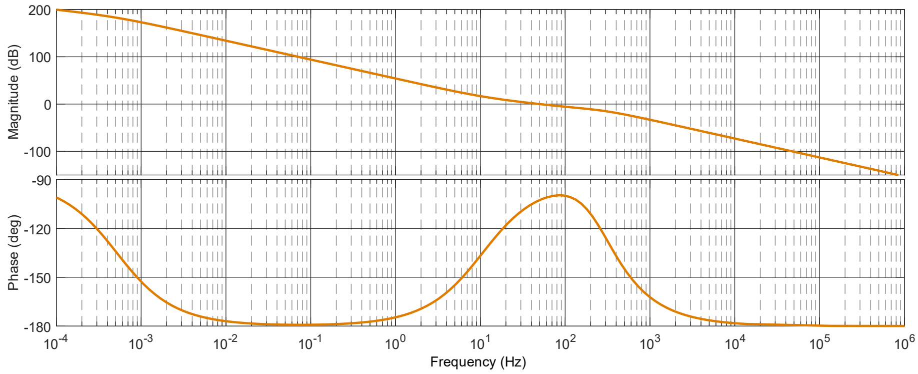

Figure 8: Loop gain in the voltage control loop around the ACM-controlled chopper converter

3. Load management for shipboard power systems

The all-electric ships are known for being 'weak' source grids. This means that such power systems possess limited generation and lower rotational inertia capacity when compared to large land-based networks (Feng et al., 2015). The consequences are translated into reduced stability margins when large portions of nonlinear and dynamic loads are included in such systems (Feng et al., 2015). Therefore, a real-time load management system might be needed to match load and generation powers (Feng et al., 2015) and enhance the system's stability under adverse situations.

In the present case of the ZEDS secondary DC Grid, converter-based resources – which present overload constraints – together with finite stored energy devices may also introduce limitations in terms of stability when supplying PLLs (for some specific mission). Thus, depending on the operational mode, the load management system should satisfy some operational constraints (Feng et al., 2015).

The real-time load management objectives can differ depending on different scenarios: operation cost reduction, profit margin maximisation, peak load contraction, and energised loads upsurge while satisfying the grid's operating constraints (Feng et al., 2012) – the latter is the target pursued for the article's zonal secondary DC-grid.

The coming sub-sections will discuss the application of the 'Multi-Agent System' (MAS) model for load management in zonal areas, but with an objective function and constraints already fixed for the local secondary loads. The MAS technology is the most popular decentralised approach, and it has already been implemented for shipload restoration, system reconfiguration, fault detection, etc. (Du et al., 2019). A centralised control scheme could also be an alternative, although it lacks adaptivity to structural changes and may become a single failure point for the entire system (Du et al., 2019).

3.1. Multi-agent system and zonal local controllers

The proposed supercapacitor secondary DC-grid has a local control system for real-time load management zonally. The load controlling behave locally in a 'Heterogeneous' way because different commands (or setting points) can be given to different agents inside the zone. Nevertheless, from the ZEDS's point of view (Figure 1),

 https://doi.org/10.24868/11136

each zone can be considered as a singular point of load – that can be supplied by port or starboard main buses – characterising a 'Homogeneous' system from that perspective. That said, the local management control can act differently in the following situations:

- **Self-restoration.** The local control can restore the normality of the secondary grid in case of failure in one of the primary chopper converters, supercapacitor banks, or 700 V main busbars. This can be accomplished by closing the bus-tie circuit breaker, changing the emergency bus selector position, and/or matching the load level with the available converter power (heterogeneous agents). This functionality is independent of the ship's automation system, so a communication failure with the port and/or starboard bus sides will not compromise performance.
- **Load limitation.** Depending on ship mission settings, the ZEDS control system will acknowledge the zone loads as a homogeneous entity and limit the total power locally – unique power indication command – if there is a need for extra power (or electrical distribution de-rated status) regarding the propulsion and PLL sub-systems. For example, in battle mode, PLLs have the highest priority, and propulsion and secondary loads can be temporarily controlled (Feng et al., 2015) to achieve the mission's requirement in a specific situation (significantly adverse ones).

The agent model formulation in ZEDS contains the physical and communication layers (Du et al., 2019). The communication network is shown in Figure 9. It becomes clear that from a local zone perspective, the agents are controlled heterogeneously, but from an outer one, the zones are treated as singular load points. It is foreseen that each zone agent locally measures its operating power and state conditions and informs the local controller (Du et al., 2019) to decide between self-restoration or load limitation actions. For the physical layer, a zonal example is illustrated in Figure 10. The local control can be chosen to determine the agent's speed or power control settings (i.e., inverter-driven motors) or turn ON/OFF lighting sections.

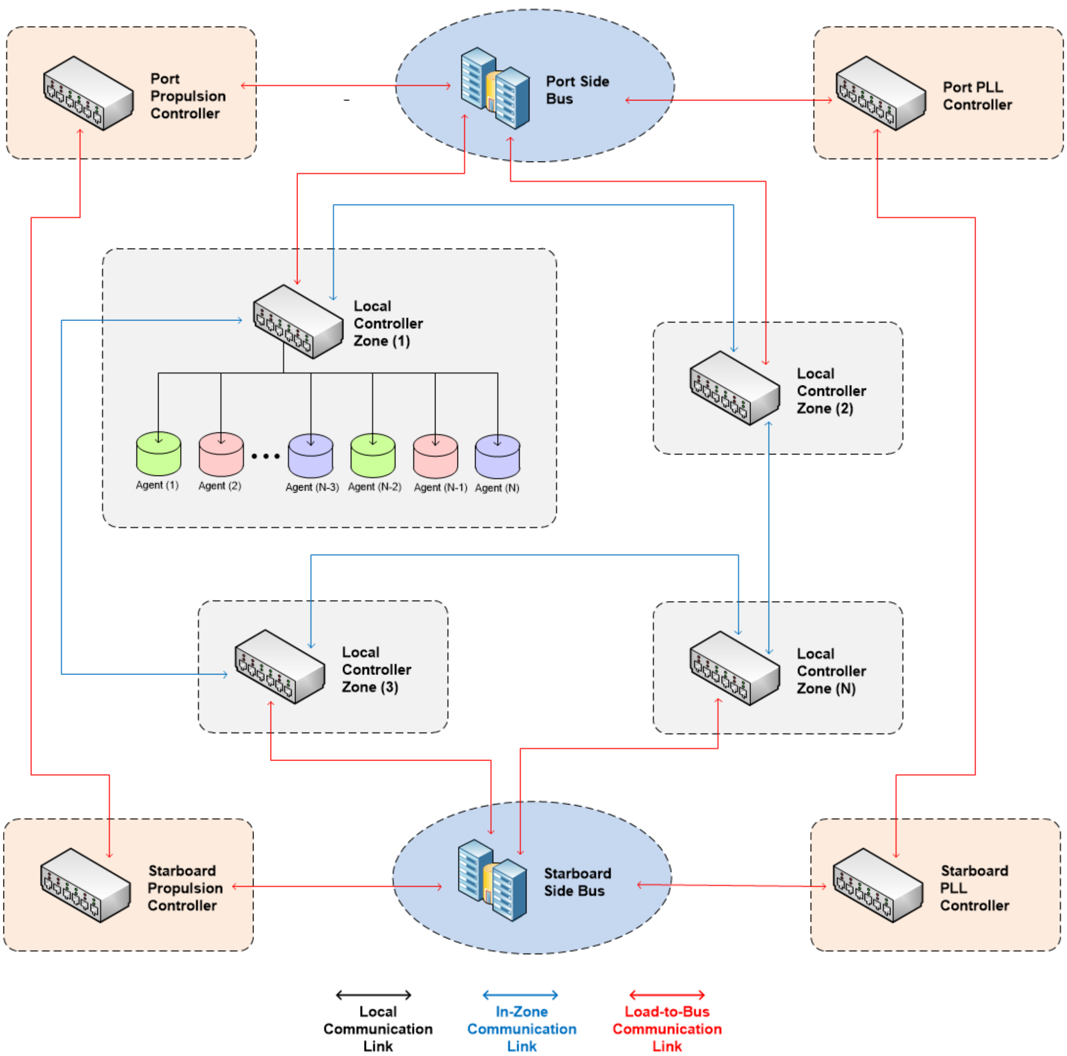

Figure 9: ZEDS communication layer regarding the MAS model for load management (Du et al., 2019)

 https://doi.org/10.24868/11136

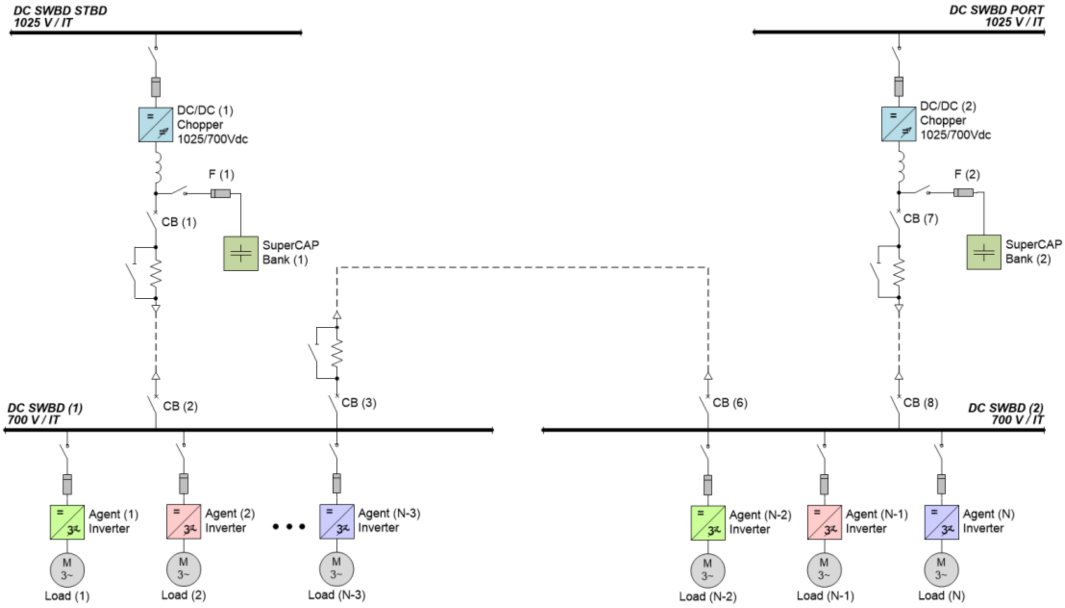

Figure 10: Zonal physical layer regarding the MAS model for load management (Du et al., 2019)

3.2. *Group objective of the secondary DC distribution*

The group objective presented from now on is related to the zonal load management's self-restoration functionality. In that case, the local controller determines each load's speed setpoints or switch status using the information provided by the secondary grid (Feng et al., 2015). In future research, the load limitation functionality would notice only the zone's total power, determining a homogeneous approach.

The ‘Seagoing Auxiliary Vessel’ secondary loads are classified into primary and secondary essential services, habitat loads, lighting, and emergency services. Primary services need to be maintained in continuous operation – the secondary ones do not necessarily; habitat services are intended to provide minimum comfort conditions for crew onboard; and emergency services guarantee minimum personal safety. In the table below, the loads in operation during Sailing mode are depicted for the group objective formulation in this sub-section.

Table 4: Seagoing Auxiliary Vessel active secondary loads during Sailing mode

Load Number	Component	Nominal Power (kW)	Efficiency (%)	Board	Service Level
1	FO Transfer Pump	2.2	0.843	DC SWBD (1)	Primary
2	LO Transfer Pump	0.75	0.796	DC SWBD (1)	Primary
3	Sea CW Pump	22	0.916	DC SWBD (1)	Primary
4	CW Pump Generator and FO Cooler 1	1.5	0.828	DC SWBD (1)	Primary
5	CW Pump Generator and FO Cooler 2	1.5	0.828	DC SWBD (2)	Primary
6	Fresh CW Pump (CW System)	11	0.898	DC SWBD (1)	Primary
7	Methanol Fuel Transfer Pump 1	1.5	0.828	DC SWBD (1)	Primary
8	Methanol Fuel Transfer Pump 2	1.5	0.828	DC SWBD (2)	Primary
9	Methanol Supply Pump Genset 1	15	0.906	DC SWBD (1)	Primary

https://doi.org/10.24868/11136

Table 4: Seagoing Auxiliary Vessel active secondary loads during Sailing mode (continuation …)

Load Number	Component	Nominal Power (kW)	Efficiency (%)	Board	Service Level
10	Methanol Supply Pump Genset 2	15	0.906	DC SWBD (2)	Primary
11	Methanol Supply Pump Aux Genset	5.5	0.877	DC SWBD (1)	Primary
12	Supply Fan 1 Engine Room	15	0.906	DC SWBD (2)	Secondary
13	Supply Fan 2 Engine Room	15	0.906	DC SWBD (1)	Secondary
14	Supply Fan Cargo Hold Room	1.28	0.75	DC SWBD (2)	Habitability
15	Supply Fan Passage Way	0.4	0.65	DC SWBD (2)	Habitability
16	Supply Fan UAV Hangar	0.4	0.65	DC SWBD (2)	Habitability
17	Supply Fan Hangar	1.28	0.75	DC SWBD (2)	Habitability
18	Exhaust Fan Galley	1.25	0.75	DC SWBD (2)	Habitability
19	CH Pump Heat Recovery 1	0.86	0.65	DC SWBD (1)	Habitability
20	CH Pump Heat Recovery 2	0.86	0.65	DC SWBD (2)	Habitability
21	Lighting 1	50	0.98	DC SWBD (1)	Lighting
22	Lighting 2	50	0.98	DC SWBD (1)	Lighting
23	Lighting Emergency	50	0.98	DC SWBD (2)	Emergency
24	Bilge Ballast Pump 1	11	0.93	DC EMERG	Emergency
25	Bilge Ballast Pump 2	11	0.93	DC EMERG	Emergency

A load priority-based approach will be applied according to the different services listed above to maximise load power for the zonal centre in Figure 2 while ensuring specified operation constraints (i.e., rated output power of the chopper converters, stable voltage performance of the supercapacitors, and continuous operation of the emergency loads). The objective function and constraints of the MAS model can be expressed as:

$$\max \sum_{a=1}^{11} P_{PRI_a}(t) + \sum_{b=1}^{2} P_{SEC_b}(t) + \sum_{c=1}^{7} P_{HAB_c}(t) + \sum_{d=1}^{2} P_{LIGHT_d}(t) \tag{1}$$

$$s.t. \sum_{a=1}^{11} P_{PRI_a}(t) + \sum_{b=1}^{2} P_{SEC_b}(t) + \sum_{c=1}^{7} P_{HAB_c}(t) + \sum_{d=1}^{2} P_{LIGHT_d}(t) \le P_{CONV} - P_{EMERG} \tag{2}$$

$$P_{PRI_a}(t) \le P_{PRI\_MEASURED_a}(t) \qquad a = 1, 2, \cdots, 11 \tag{3}$$

$$P_{PRI_a}(t) = \alpha . P_{PRI\_NOMINAL_a} \qquad \alpha \in \{0, 0.4, 0.5, 0.6, 0.7, 0.8, 0.9, 1\} \tag{4}$$

$$P_{SEC_b}(t) \le P_{SEC\_MEASURED_b}(t) \qquad b = 1, 2 \tag{5}$$

$$P_{SEC_b}(t) = \beta . P_{SEC\_NOMINAL_b} \qquad \beta \in \{0, 0.4, 0.6, 0.8, 1\} \tag{6}$$

 https://doi.org/10.24868/11136

$$P_{HAB_c}(t) = \gamma . P_{HAB\_MEASURED_c}(t) \qquad c = 1, 2, \cdots, 7 \ | \ \gamma \in \{0, 1\} \tag{7}$$

$$P_{LIGHT_d}(t) = \delta . P_{LIGHT\_MEASURED_d}(t) \qquad d = 1, 2 \ | \ \delta \in \{0, 1\} \tag{8}$$

where $P_{PRI\,a}(t)$ is the active power of the Primary load 'a', $P_{SEC\,b}(t)$ is the active power of the Secondary load 'b', $P_{HAB\,C}(t)$ is the active power of the Habitability load 'c', $P_{LIGHT\,D}(t)$ is the active power of the Lighting load 'd', P_{CONV} is the total available power for the primary chopper converters, and P_{EMERG} is the reserved power for the Emergency loads.

The load priority-based approach is based on thirteen steps that can reduce, for instance, the secondary base load up to 17% (from its initial condition) when the ship is operating in Sailing mode. The power steps reduction are not fixed values but somewhat dependent on the priority sequence disclaimed in Table 5 – based on the parameters α, β, γ, and δ, from Equations 1-8. During regular operation, the above parameters are equal to one. The sequence of step events is based on the highest priority given to Primary loads and the lowest ones to Habitability. In any case, the load management controller never affects the emergency loads when seeking self-restoration. In Figure 2, it can be seen that there is a dedicated battery system for powering the emergency busbar in case of energy loss in the zone.

Table 5: Load priority-based approach constant values

Load Step	**Primary (α)**	**Secondary (β)**	**Habitability (γ)**	**Lighting (δ)**
1st	1	1	0	1
2nd	1	0.8	0	1
3rd	1	0.6	0	1
4th	1	0.4	0	1
5th	0.9	0.4	0	1
6th	0.8	0.4	0	1
7th	0.7	0.4	0	1
8th	0.6	0.4	0	1
9th	0.5	0.4	0	1
10th	0.4	0.4	0	1
11th	0.4	0	0	1
12th	0	0	0	1
13th	0	0	0	0

4. Zonal main converter failure study case

4.1. Study case description

This section presents a study case where the chopper converter 'DC/DC (1)' completely fails. We limit ourselves to the situation where the three inverter legs of the converter fail – although partial failures are also feasible. First, the modelling of the components in the study case will be discussed. Next, the load management strategy and algorithm already mentioned to mitigate this failure will be introduced, thereby avoiding the blackout.

 https://doi.org/10.24868/11136

We simulate the failure event in the Matlab-Simulink environment, and show the results of the study case from different perspectives: switchboard busbar voltages, service level component loads and component currents.

4.2. Component modelling

For the study case, a logic load management algorithm that runs at a frequency of 1000 Hz is applied. For this particular simple case, 1000 Hz is more than sufficient. Although a lower operating frequency is also feasible due to the higher time constant dynamics that the supercapacitors provide, high-frequency load management is beneficial in situations with small supercapacitors-load power ratios or low time constant dynamics.

First, the DC/DC converters and supercapacitors are modelled precisely as described above in Section 2.2 using the Simscape Electrical toolbox. Two types of loads are considered: 1) constant power loads are used for (emergency) lighting, CH heat recovery pumps, and bilge ballast pumps – those loads have a power setpoint P^* which in this study case is either its nominal value or 0 when it is OFF; 2) the rest of the loads in Table 4 are modelled as multiple elements (i.e., namely a direct torque control space vector pulse width modulated (DTC SVPWM) controller, inverter, an induction motor and the mechanical pump element). The base equation for the pump speed and pump power relationship is defined as:

$$P \sim \omega^3 \tag{9}$$

For the actual study case, we formulate this as the following third-order polynomial, illustrated in Figure 11 – which is scaled for each pump with nominal speed and power:

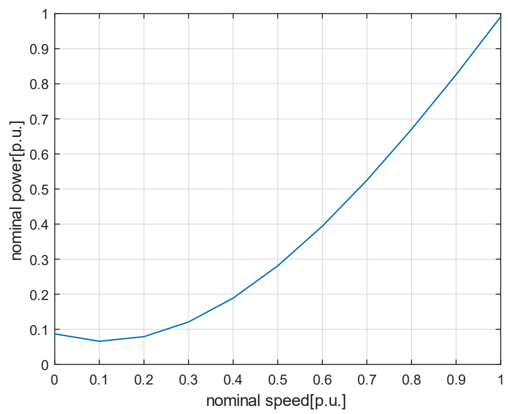

Figure 11: Nominal pump speed vs. power curve

The input of the motor load is the speed setpoint ω^*, provided in all the modelled pump elements, illustrated in Figure 12. For the sake of clarity, feedback signals have been omitted.

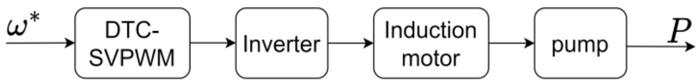

Figure 12: Simulated pump motor control blocks

Subsequently, the pump motor controller is placed in a feedback loop control, illustrated in Figure 13, to compensate for modelling errors and offset disturbances. The input of this feedback loop is a power reference setpoint P^* with a conversion to ω^* for the pump, according to Figure 11. A feedforward element is added so that the PI controller only has to compensate for the *error* = $P^* – P$. Finally, power and speed values are normalised, which is crucial as the pump is highly non-linear and non-adaptive.

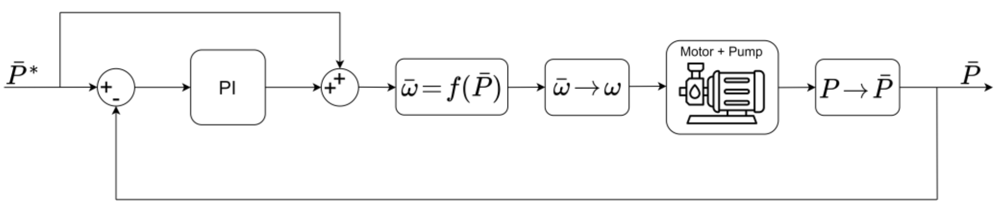

Figure 13: Pump motor control feedback loop

4.3. Logic control algorithm

The logic control algorithm consists of two main parts: 1) the closing of the bus-tie circuit breaker and 2) the load management algorithm.

Table 6: Bus-tie breaker trigger time for several converter overload currents and voltage thresholds

Overload Factor ($_xI_n$)	**Overload Current [A]**	**Trigger Time 680 Vdc [sec.]**	**Trigger Time 660 Vdc [sec.]**	**Trigger Time 640 Vdc [sec.]**
1.2	306	12.718	28.467	48.112
1.5	382.5	4.531	9.909	15.712
2	510	1.949	4.528	7.195
3	765	0.691	1.949	3.228
4	1020	0.273	1.109	1.949

For closing the bus-tie breaker ‘CB (3)’, three conditions must be satisfied:

1. The switchboard ‘SWBD (1)’ filtered voltage value is below the voltage threshold (i.e., 680, 660, or 640 Vdc) for 0.01 seconds;
2. There is sufficient time to close the bus-tie circuit breaker. This is based on the resultant time constant of Table 6 that depends on the overload current factor and the voltage threshold selected – the resultant time must be greater than 3 seconds; otherwise, the breaker cannot be closed;
3. There are no faults/error alarms from components ‘CB (1)’, ‘CB (2)’, ‘F (1)’ and ‘SuperCAP (1)’.

When all conditions are assumed to be met, and a converter failure event occurs, the voltage decreases. The bus-tie circuit breaker is triggered when the voltage threshold is crossed. It closes in two steps, as described in section 2.1. If the ‘DC/DC (2)’ converter is still in overload condition, load management must be applied.

Load management follows the principle of reducing low-priority loads first by adjusting the factors α, β, γ, and δ, weight parameters and shedding loads. For the study case, in particular, presented in Table 5, the appropriate steps must be found to maximise loads. However, the converter's nominal power must not be exceeded, which is done by evaluating the steps until this condition (Equation 2) is satisfied.

The developed logic load management is generic and not limited to the study case. It assumes that the loads are operating at feasible values of α, β, γ, and δ, as defined in Equations 4-8. It is essential to highlight the partial overlap of reducing the secondary and primary service level loads. All secondary service level loads with $\beta > 0.4$ are first reduced to 0.4, after which any primary service level load with $\alpha > 0.4$ are reduced to 0.4. Once done, then values of $\beta = 0.4$ are reduced to $\beta = 0$. Finally, values of $\alpha = 0.4$ are reduced to $\alpha = 0$.

Using the service level priority order and the inequality of Equation 2, we can convert this into (nested) switch statement(s), creating a long list of cases. The load management algorithm is explained in Pseudocode 1, but instead of using switch case statements, we use a while loop for the sake of clarity and conciseness – but the principles are the same. The main objective of maximising the loads whilst not exceeding the converter's nominal power limit has become the condition for exiting the while loop.

4.4. Results and discussion

Figure 14 illustrates the busbar voltages of the switchboards ‘DC SWBD (1)’ and ‘DC SWBD (2)’. Additionally, the main events are depicted as vertical lines corresponding to their time of occurrence. It is started in regular operation in which the loads have the nominal operating points indicated in Table 4. The (emergency) lighting loads are an exception, with loads 21, 22 and 23 operating at 55%, 55% and 30% of their nominal power, respectively. The converter ‘DC/DC (1)’ fails at approximately 2.7 seconds, disabling it altogether. As a result, the voltage of ‘DC SWBD (1)’ decreases as ‘SuperCAP (1)’ discharges to supply energy to the loads. At an instant of 5.3 seconds, the first part of the logic algorithm is triggered due to the voltage threshold crossing. All criteria for closing the bus-tie circuit breaker are met, and the first switch closes. Now, ‘DC SWBD (1)’ and ‘DC SWBD (2)’ are connected, and both supercapacitor banks are in the same grid. At this point, the ‘DC/DC (2)’ converter supplies the loads located in this zone of the ship entirely. Although the voltage in ‘DC SWBD (1)’ temporarily increases again, it is of short duration. Both switchboard voltages decrease again due to the overload condition of the ‘DC/DC (2)’ converter and the discharging of the supercapacitors. At instant 8.3 seconds, and as intended, the bypass switch of the bus-tie circuit breaker closes. With the voltages in both switchboards still decreasing, the second stage of the logic algorithm is activated as the voltage threshold is crossed again at 11.3 seconds. At this point, Figure 14 illustrates two possibilities: 1) apply load management and restore the voltage to its nominal value, or 2) do not apply load management and eventually the voltage will lead to the failure of 'DC/DC (2)' converter due to under-voltage trip, resulting in a total zonal blackout. The remainder of this paper assumes that load management is selected and applied.

Pseudocode 1: Simplification of logic load management algorithm

Algorithm 1: load management

input: load power measurements vector: $P_{measured}$
output: load reference setpoints vector: U_{ref}
Identify weights factors $\alpha, \beta, \gamma, \delta$ for each individual load *i*. Assume load setpoints operate at weight factor $\alpha_i, \beta_i, \gamma_i, \delta_i$ of their nominal powers $P_{nom,i}$ respectively. They are placed in vectors $\vec{\alpha}, \vec{\beta}, \vec{\gamma}, \vec{\delta}$
define U_{ref} and copy $P_{measured}$ into it
define '*condition1*' as $\sum P_{measured} \leq P_{nom.converter}$ - $P_{emergency}$
while *condition1* == false
  if any γ in $\vec{\gamma} > 0$
    set all γ in $\vec{\gamma}$ to 0; update corresponding habitability power reference setpoints to 0 in U_{ref}
    continue
  if any β in $\vec{\beta} > 0.4$
    decrease all β in $\vec{\beta}$ which have value equal to max($\vec{\beta}$) by one step (see Eq. 6) but not smaller than 0.4; corresponding secondary service level power reference setpoints to $\beta_i \cdot P_{nom,i}$ in U_{ref}
    continue
  if any α in $\vec{\alpha} > 0.4$
    decrease all α in $\vec{\alpha}$ which have value equal to max($\vec{\alpha}$) by one step (see Eq. 4), but not smaller than 0.4; update corresponding primary service level power reference setpoints to $\alpha_i \cdot P_{nom,i}$ in U_{ref}
    continue
  if all β in $\vec{\beta}$ == 0.4
    set all β in $\vec{\beta}$ to 0; update corresponding secondary service level power reference setpoints to 0 in U_{ref}
    continue
  if all α in $\vec{\alpha}$ == 0.4
    set all α in $\vec{\alpha}$ to 0; update corresponding primary service level power reference setpoints to 0 in U_{ref}
    continue
  if any δ in $\vec{\delta} > 0$
    set all δ in $\vec{\delta}$ to 0 and update corresponding lighting power reference setpoints to 0 in U_{ref}
    continue
  if all values in $\vec{\alpha}, \vec{\beta}, \vec{\gamma}, \vec{\delta}$ == 0
    break
for load No. *i* =12, … ,22, let power reference setpoints unchanged in U_{ref}. For load No. *i*= 1, … ,11, perform an additional in-place power setpoint reference conversion to their respective nominal value.

Figure 15 depicts the cumulative sum of each service level load over time. The initial 2 seconds represent the motor loads' starting process in the zone. Although the failure event occurs at around 2.7 seconds, this is not reflected in the loads over time. This indicates that the inclusion of supercapacitor functions as expected. Secondly, the low-priority loads are either reduced or shed during load management adjustment. For instance, habitability service level loads are shut down, and primary essential service loads are reduced to 50%. In succession, the highest priority service level loads remain operational.

Finally, Figure 16 illustrates the current flows of each power component. In regular operation, it is evident that there is negligible current flow from the supercapacitors, with all power supplied from the two chopper converters. After the failure event, one can observe that 'SuperCAP (1)' immediately takes over. Subsequently, at 5.3 seconds, the closure of the bus-tie circuit breaker illustrates two peaks in current flow, as depicted in Figure 3. The current flow through 'SuperCAP (1)' briefly becomes negative, charging it and resulting in a short-duration voltage increase, as observed in Figure 14. At an instant of 8.3 seconds, 'SuperCAP (1)' charges for a short duration due to the current outflow of 'SuperCAP (2)'. Lastly, it is notable that the short high transients at the moment of enabling the load management in Figure 16 (i.e., sudden motor deceleration) are effectively filtered out by ‘SuperCAP (1)’ and ‘SuperCAP (2)’ – meaning higher stability for the grid.

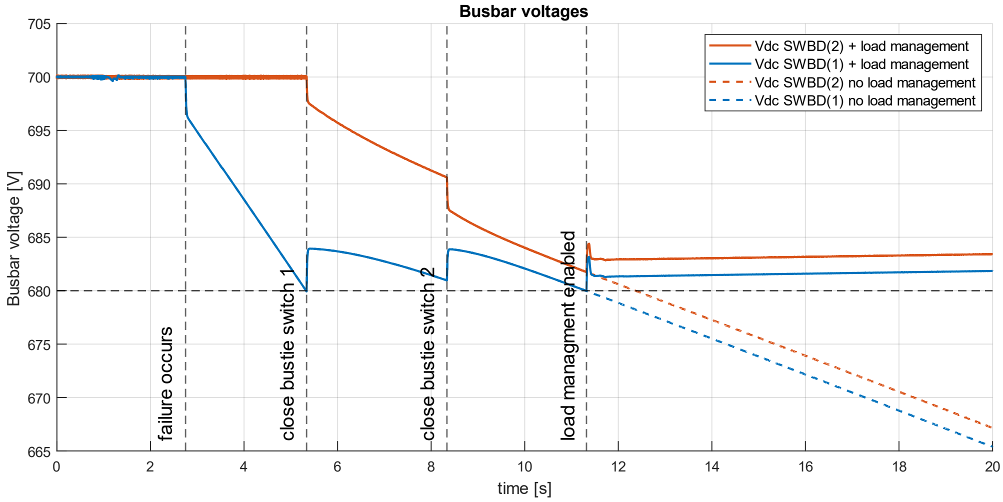

Figure 14: Study case zonal switchboard busbar voltages over time

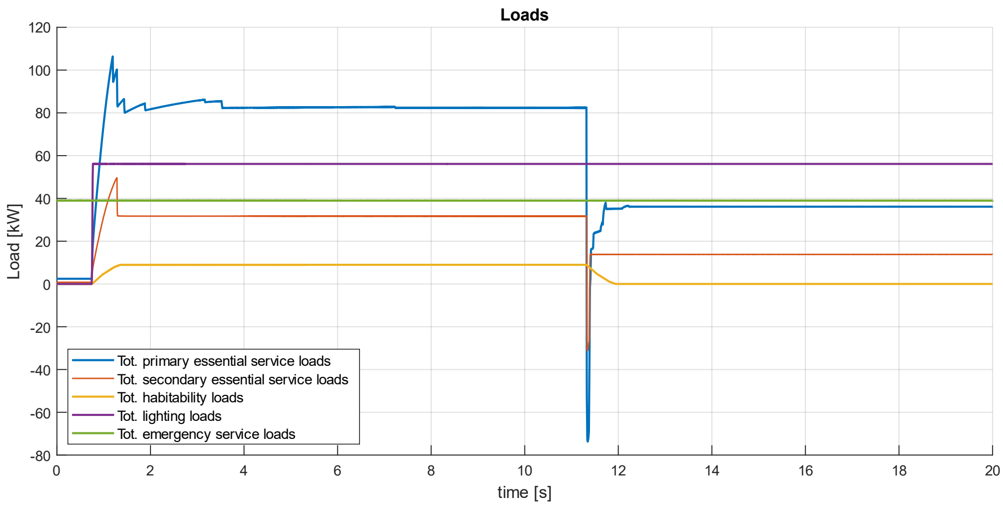

Figure 15: Service level component load sums over time

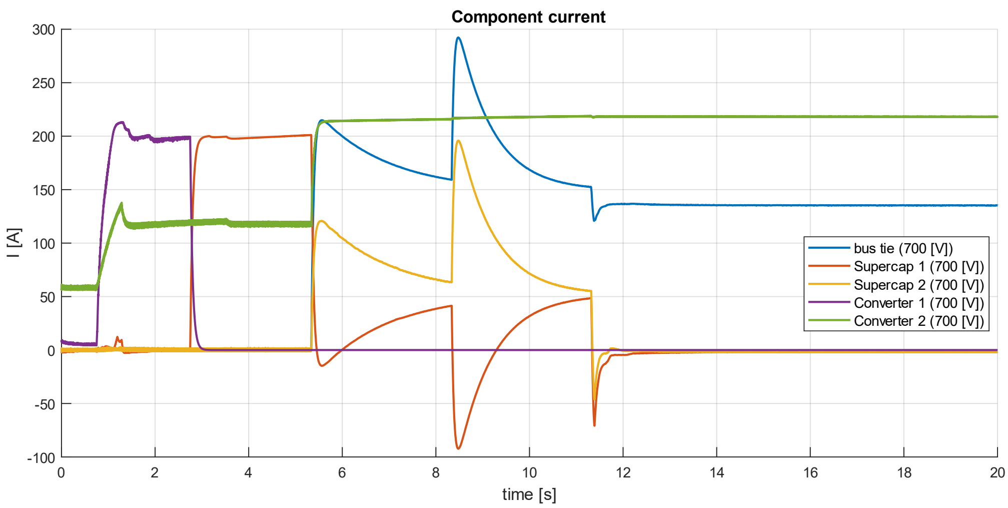

Figure 16: Power system components’ current over time

The presented results come from ideal simulations in Matlab-Simulink environment. Constant nominal power loads are used, with some being reduced using a fixed set of weights or shut-down signals. Although the power components have been modelled in great detail, some imperfections are inevitable due to some assumptions and simplifications. To address these imperfections, the pump setpoint control is placed in a PI-control feedback loop for mitigation. This compensates for model imperfections and disturbances. However, this approach has limitations since the pump dynamics are highly non-linear. Despite normalising the inputs and outputs, the feedback controller is still linear and, therefore, requires cautious tuning.

Furthermore, while the logic controller design is applicable outside the study case, it is notable that assuming (approximate) constant loads is, of course, limiting with more dynamic loads expected in practice. However, the logic load management algorithm runs at a high frequency, which could mitigate the impact of such dynamic loads.

5. Conclusions

This work proposes a strategy based on load priority to enhance survivability in zonal DC-grids. A study case based on the 'Seagoing Auxiliary Vessel' was proposed to demonstrate the effectiveness of the priority-based strategy. The strategy comprises a two-stage solution in which voltage threshold triggers first enable the closing of a bus-tie circuit breaker followed by the load adjustments to ensure maximum continuous operation of high-priority loads. The study case featured a chopper converter failure in a zonal DC grid with supercapacitors. The results demonstrated that the high-priority loads continued to operate, the system's voltage was recovered (or kept at operational levels), and converter tripping due to under-voltage setting was prevented.

Incorporating a power reserve can yield faster voltage restoration and power quality improvements in future work. Furthermore, application in practice, such as dredging operations, can provide valuable insights. Finally, combinations with interzonal algorithms can be explored.

Acknowledgements

This work is part of the subsidy scheme for R&D mobility sectors for the MENENS project, which is funded by the Netherlands Enterprise Agency (RVO).

References

Bosich D., Chiandone M., Sulligoi G., Tavagnutti A. A. & Vicenzutti A.: "High-Performance Megawatt-Scale MVDC Zonal Electrical Distribution System Based on Power Electronics Open System Interfaces", IEEE Transactions on Transportation Electrification, vol. 9, no. 3, pp. 4541-4551, Sept. 2023.

Deroualle J. J., Vinks S.: "Supercapacitors for Enabling Mechanical Circuit Breakers in Shipboard Zonal Secondary DC-Grids", IEEE 6th International Conference on DC Microgrids, ICDCM 2024.

Du W., Yang G., Pan C. & Xi P.: "A Heterogeneous Multi-Agent System Model with Navigational Feedback for Load Demand Management of a Zonal Medium Voltage DC Shipboard Power System", IEEE Access, vol. 7, pp. 148073-148083, 2019.

Erickson R. W. & Maksimović D.: "Chapter 18: Current-Programmed Control", Fundamental of Power Electronics, 3rd ed., Cham, SZ: Springer, 2020, pp. 725-804.

Feng X., Butler-Purry K. L. & Zourntos T.: "Multi-Agent System-Based Real-Time Load Management for All-Electric Ship Power Systems in DC Zone Level", IEEE Transactions on Power Systems, vol. 27, no. 4, pp. 1719-1728, Nov. 2012.

Feng X., Butler-Purry K. L. & Zourntos T.: "A Multi-Agent System Framework for Real-Time Electric Load Management in MVAC All-Electric Ship Power Systems", IEEE Transactions on Power Systems, vol. 30, no. 3, pp. 1327-1336, May 2015.

"IEEE Recommended Practice for 1 kV to 35 kV Medium-Voltage DC Power Systems on Ships", IEEE Std. 1709-2018 (Revision of IEEE Std. 1709-2010), pp.1-54, 7 Dec. 2018.

Qazi S. et al.: "Powering Maritime: Challenges and prospects in ship electrification", IEEE Electrification Magazine, vol. 11, no. 2, pp. 74-87, June 2023.

Xu L. et al.: "A Review of DC Shipboard Microgrids – Part I: Power Architectures, Energy Storage, and Power Converters", IEEE Transactions on Power Electronics, vol. 37, no. 5, pp. 5155-5172, May 2022.